THE AMERICAN SOCIETY OF MECHANICAL ENGINEERS
345 E. 47th St., New York, N.Y. 10017

94-GT-14

THREE-DIMENSIONAL NAVIER-STOKES PREDICTION OF HEAT TRANSFER WITH FILM COOLING

J. M. Fougères and R. Heider
Turbine Aero and Cooling Department
Snecma
Moissy-Cramayel, France

ABSTRACT

Three-dimensional Navier-Stokes calculations have been performed on various geometries in the presence of discrete-hole injection. The quality of the aerodynamic and thermal predictions of the flow is assessed by comparison to experiments.

The code used for the calculations is developed at ONERA and has previously been presented by various authors (Billonnet et al., 1992). It solves the unsteady set of three-dimensional Navier-Stokes equations, completed by a mixing-length turbulence model, using a finite volume technique.

The multi-domain approach of the code has facilitated the treatment of this type of geometry. The injection holes are discretized on cylindrical subdomains which overlap the mesh of the main flow.

Two applications of the code are presented in this paper. First, a calculation was performed on a row of hot jets injected into a flat plate turbulent boundary layer. Secondly, the code was tested on a plane nozzle guide vane grid with multiple injections. Heat transfer rates, temperature and velocity profiles are compared to experimental data.

NOMENCLATURE

D	diameter of the hole
H	heat transfer coefficient $H = \Phi/(T_\infty - T_w)$
M	blowing ratio = $(\rho V)_j/(\rho V)_\infty$
s	curvilinear coordinate on the blade
u	streamwise component of velocity vector
V	magnitude of velocity vector
x	streamwise coordinate
y	coordinate normal to the wall
y^+	dimensionless distance to the wall
z	spanwise coordinate
δ	boundary layer thickness
Φ	heat flux
κ	Von Karman constant
μ	molecular viscosity
μ_t	eddy viscosity
ρ	density

Subscripts

E	end of transition
j	injection
ps	pressure side
S	start of transition
ss	suction side
w	wall
∞	free stream

INTRODUCTION

Industrial Objectives

The search for better performance for air plane engines has led to higher gas temperatures in the first stages of modern turbines. In these operating conditions, the turbine blades need to be cooled to ensure their integrity and achieve the life objectives.

Discrete jet film-cooling is one of the techniques used to protect the blades and endwalls, which are particularly thermally exposed. The best compromise between admissible metal temperature and aerodynamic efficiency becomes a major objective in cooled turbine blade design.

This goal is within engine manufacturers' reach because of more powerful super computers which now allow global and representative 3D computations.

Presented at the International Gas Turbine and Aeroengine Congress and Exposition
The Hague, Netherlands — June 13–16, 1994

Coolant Injection and Heat Transfer by CFD

In the past five years, modified 2D boundary layer codes attempted to predict heat transfer and losses resulting from coolant injections. The model of injection and dispersion presented by Haas et al. (1991) was purely two-dimensional. Distorted profiles were injected behind the injection region and additional terms, representing the 3D effects, were added to 2D boundary layer equations. Another approach was presented by Kulisa et al. (1991). This calculation is based on iterative couplings between a 3D jet model and a 2D boundary layer code. The jet is calculated in an external flow taking into account the presence of the jet and average spanwise terms are introduced in the 2D boundary layer code. The numerous constants of these models need to be calibrated by an experimental database. This aspect prevents application of the codes to new coolant configurations.

Recent work, using 3D Navier-Stokes calculations, have appeared in the literature. Codes, using mixing-length-type turbulence models, are able to compute accurate aerodynamics, provided that the grid refinement in the boundary layer region be sufficient. The discretization should extend to the viscous sublayer. This has been demonstrated by Wegener et al. (1992) for a low pressure turbine and by Couaillier et al. (1991) for the case of a transonic fan.

As stated by other authors, accurate computation of heat transfer is far more critical to obtain, even using 2D codes (Chanez et al., 1993). An important mesh refinement, leading to values of $y+$ of the order of unity for the near wall mesh cells, is necessary according to many authors. Encouraging heat transfer predictions on 3D cases could thus be achieved by Ameri and Arnone (1991) on the low pressure Langston cascade or by Boyle and Giel (1992) on the high pressure guide vane of the Space Shuttle main engine using grids that were highly refined (y^+ ranging from 0.6 to 2.5) but also of remarkable regularity and orthogonality.

A common issue to lower computational costs is to use wall functions to model the eddy viscosity within the viscous sublayer. This technique although providing sometimes accurate aerodynamic predictions should be applied to thermal predictions with care since they may be far from satisfying (Choi and Knight, 1991).

Heat transfer and skin friction can only be computed with some success if the laminar-turbulent transition is correctly modelled or specified (Abu-Ghannam and Shaw, 1980). If this is the case, mixing-length models are as competitive as two equation models in predicting heat-transfer according to Ameri and Arnone (1992).

Roth et al. (1992) used a thin-layer Navier-Stokes solver to compute the Fearn and Weston (1974) injection cases. However, these cases did not present a jet in interaction with a wall so heat transfer at the wall was not estimated. This aspect has been treated by Leylek and Zerkle (1993) on an experimental apparatus studied by Pietrzyk et al. (1989). The full geometry, containing the plenum chamber, the hole and the flow-path, has been meshed. Fair agreement was obtained between the calculated and experimental adiabatic effectiveness obtained on this flat plate. Dorney and Davis (1993) studied, with an unsteady 3D Navier-Stokes code, the effects of film cooling hole locations to diminish the impact of combustor hot streaks in a one stator-one rotor configuration. These results, though no comparison was made with experiments, show that current unsteady three-dimensional film cooling design will be next in coming.

Present Contribution

Two computations are presented in this paper with the aim of analysing the capability of the 3D Navier-Stokes code to predict heat transfer in presence of discrete hole injections. First, a 3D calculation on a row of hot jets injected in a flat plate turbulent boundary layer is presented. Second, a 3D computation of the flow between two stream-surfaces, spaced one hole pitch apart, around a plane cascade nozzle guide vane with multiple injections is presented.

The implementation of the computations with respect to the particularities of the employed grid, boundary conditions, turbulence model and initialization technique is discussed. A description of the test facilities and measurement techniques, then, discusses the type of experimental data available. Results are then analysed with respect to heat transfer, temperature, velocity and general flow features.

SOLVER CHARACTERISTICS

The 3D Navier-Stokes code used for the presented computations is developed at ONERA (Couaillier et al., 1992) and intensively used at SNECMA for turbomachinery applications. The code solves the unsteady set of three-dimensional Navier-Stokes equations by means of Ni's Lax-Wendroff scheme (Ni, 1982). An implicit residual smoothing step is used to accelerate the convergence towards a steady solution. A mixing-length turbulence model formulated by Michel et al. (1969) and adapted to 3D cases by Cambier and Escande (1990) is used to compute the eddy-viscosity. The multi-block structure of the code allows an optimal discretization of complex shapes. Information transfer across adjacent or overlapping boundaries is handled by means of trilinear interpolation. The numerical aspects of the scheme have already been described on different occasions (see e.g. Heider et al., 1993).

EXPERIMENTAL TEST FACILITIES

The computations were validated on data banks obtained on two test facilities. The first one is a fundamental study of a row of hot jets, injected in the boundary layer of a flat plate, which was carried out at the CEAT-Poitiers (France). The second one is a film cooled high pressure nozzle guide vane, tested in the isentropic

Light Piston Compression tube at the Von Karman Institute (Belgium).

Flate Plate

A complete description of the first experimental apparatus has been presented by Foucault et al. (1992). The experiments have been performed in a subsonic Eiffel type wind tunnel. The flow path has a rectangular cross section (0.3mx0.4m) and is one meter long.

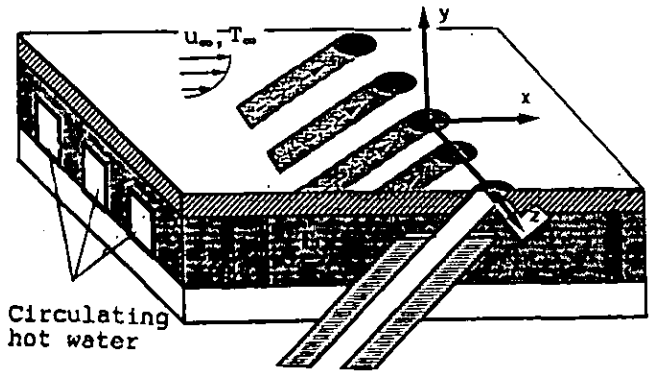

Figure 1. CEAT-Poitiers test apparatus.

The air, heated at 333K in a compressor, is injected at various blowing ratios into the main stream (u_∞=32m/s), at the atmospheric temperature and pressure, by a row of five 45° holes. The film-hole length-to-diameter ratio is 20. The row of holes, with a pitch-to-diameter ratio of 3, is placed at 0.5m from the entrance of the flow path. In the injection region, the turbulent boundary layer thickness-to-diameter ratio is equal to 2. The code was tested for a main stream temperature of 298K and for a blowing ratio equal to 0.66 at a coolant-to-gas density ratio of 0.89.

Laser anemometry and a cold wire system were used to acquire detailed measurements of the velocity components and tempereture in the flow. The temperature on the flate plate was deduced from the measurements of an infra-red camera. The internal surface of the flat plate is maintained at 333K by a system of circulating hot water (fig. 1). Uniformity and constancy of this internal temperature were controlled by thermocouples. The heat transfer was estimated with the resulting temperature gradients between the external surface of the flat plate and the internal one. Resulting flux was given with an uncertainty of 5%.

Film Cooled Plane Nozzle Guida Vane

The second test apparatus has been presented by Arts and Lapidus (1992). The experimental investigation was performed in the CT2 Von Karman Institute facility. A film cooled nozzle guide vane was mounted in a linear cascade configuration, consisting of five airfoils. Each cooling location consists of two rows of staggered holes. The diameter of the holas is 0.5mm and the pitch is equal to three diameters. The short duration tests were conducted with various values of free stream total pressure, turbulence level and pressure ratio. Different cooling locations, blowing ratios and cooling temperatures were tested on the pressure and suction side of the blades.

The central airfoil is interchangeable and was equipped either for aerodynamic or heat transfer study .

Local wall static pressure and upstream total pressure measurements provided the isentropic Mach number only for the uncooled configurations. A transient measurement technique determined the spanwise averaged wall heat flux along the airfoil surface. The uncertainty on the experimental heat transfer coefficients is 7%. The selected operating conditions for our computation are shown in table 1.

measured free stream conditions	
total pressure	3.40 bar
total temperature	426 K
exit Mach number	0.86
free stream turbulence	4%
wall temperature	297 K

measured coolant conditions	suction side	pressure side
total pressure	3.13 bar	3.35 bar
total temperature	292.5 K	294.5 K
blowing ratio	0.700	0.900

Table 1. Nozzle vane test operating conditions.

IMPLEMENTATION OF THE COMPUTATIONS

Grid Generation

Both geometries consist of a main-stream flow-path and injection holes.

The main-stream grid is generated in a usual way. For the flat plate (fig. 2a), it consists of a single H-type domain (83839 points). The turbine blade is discretized, on a one hole-pitch thick stream layer (fig. 3), in three blocks (196281 points)(fig. 4). The first block, upstream of the blade, consists of an H-type mesh. The mesh around the blade is an O-type. The third block, downstream of the blade, consists of a H-type mesh. This mesh is generated by stacked 2D grids, each of which has been submitted to an optimizing algorithm (Jacquotte and Cabello, 1988). Both grids are refined in near-wall and injection regions.

The injection holes are meshed on cylinders which overlap the main stream grid. Each cylinder is composed of 20274 points distributed among two subdomains : an outer O-type grid which is pinched on its inner boundary at four corners thus allowing the location of an inner H-type grid (fig. 2b). The overlapping technique has been chosen because it allows an automatic meshing of the holes. The only parameters to be specified are the hole radius, the injection location on the blade and its angle in the engine frame.

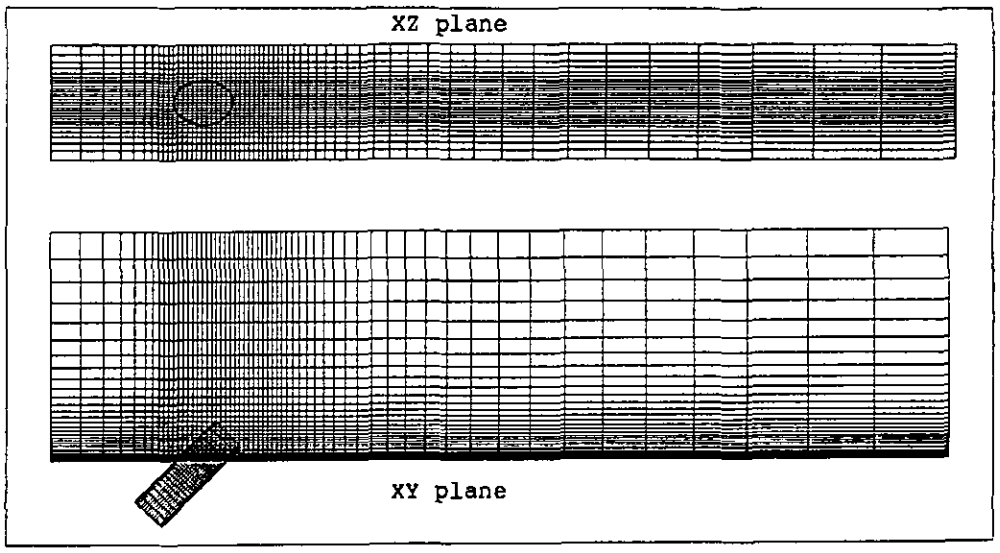

a/ Calculation domain

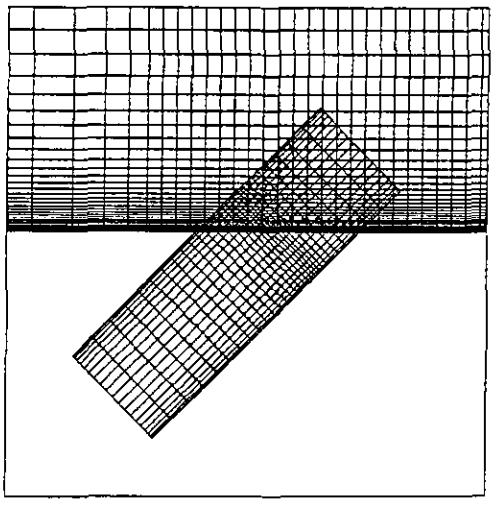

b/ injection zone

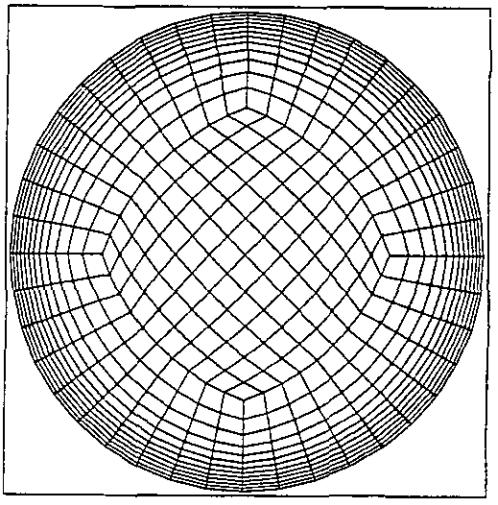

cylinder cross section

Figure 2. Flat plate and injection cylinder meshes.

Boundary Conditions

Once the grid is generated, an algorithm is performed for the boundaries of overlapping domains to determine which points belong to a fluid-fluid boundary and which ones are located on a wall.

A zero velocity condition with specified wall temperature is applied on all solid surfaces including the hole walls. On adjacent or overlapping boundaries, trilinear interpolation of the flow variables is performed.

This technique is conservative for matching grid points. Therefore fluid-fluid boundaries are conceived in a way that grid points coincide wherever possible. On overlapping or periodic boundaries, the interpolation error is minimized by an important mesh density.

Total pressure, total temperature and flow angle are specified on all injecting boundaries, static pressure is imposed on downstream boundaries since the flow is subsonic.

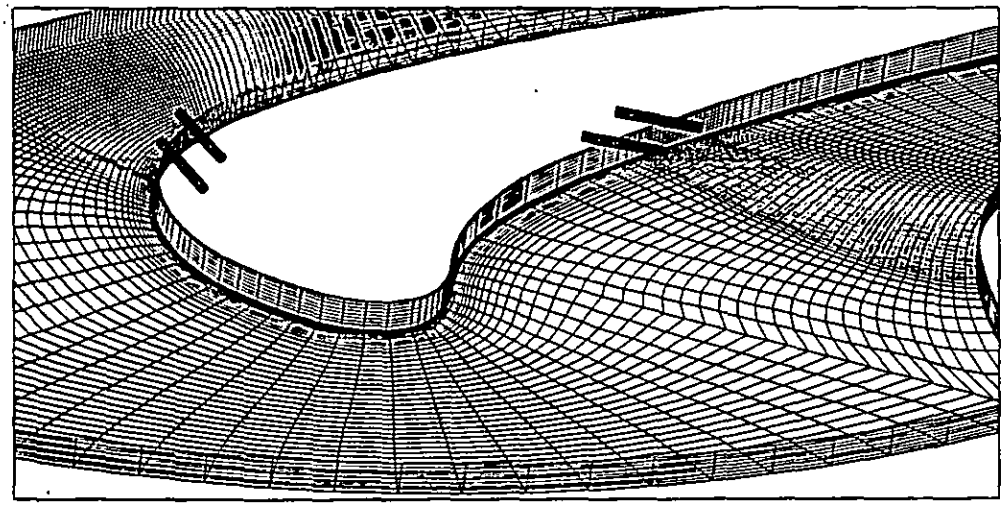

Figure 3. Three-dimensional view of the stream layer mesh.

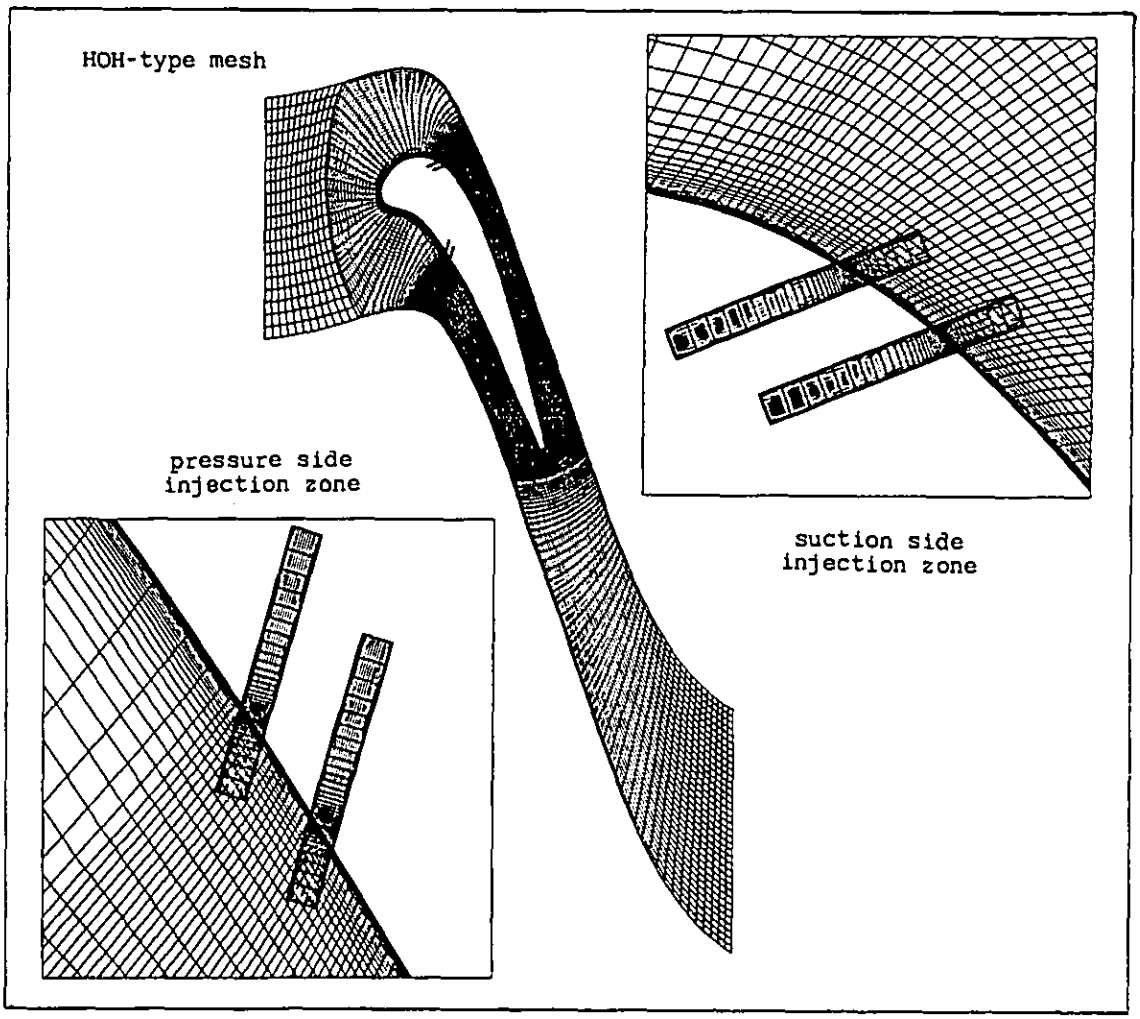

Figure 4. Cross section mesh of airfoil and cooling holes.

Adaptation of the Turbulence Model

The eddy viscosity coefficient is given by Michel's mixing length model (Cambier and Escande, 1990) :

$$\mu_t = \rho l^2 F^2 \mid \Omega \mid$$

$\mid \Omega \mid$ denotes the magnitude of the vorticity and the mixing length l is given by :

$$l = 0.085\ \delta \tanh [(\kappa d)/(0.085\delta)]$$

where d denotes the distance normal to the nearest wall. The boundary layer thickness (δ) is defined as the distance to the wall where the vorticity magnitude ratio $\mid \Omega \mid / \mid \Omega \mid_{max}$ is more than some value Ω_0.

The damping factor F is evaluated by the following relation :

$$F = 1 - \exp[-\sqrt{\zeta}/(26\kappa)]$$

$$\text{with } \zeta = \rho\, l^2\, (\mu + \mu_t)/\mu^2 \mid \Omega \mid$$

The distance to the nearest wall accounts for the presence of the injection holes which are considered as walls by the code. The distance and, therefore the eddy viscosity, inside the orifice of injection is different from zero.

The calculation of a boundary layer thickness in a flow perturbated by jets has no more real sense. However, the magnitude of the vorticity, and therefore the distance to the wall δ, accounts for the presence of the jets. With Michel's definition, δ is considered as a reference length for these cases of injection. The threshold value Ω_0 has been calibrated at 0.003 for the injection cases. The process to determine the boundary layer thickness δ, described above, is applied everywhere except for the cylindrical injection domains.

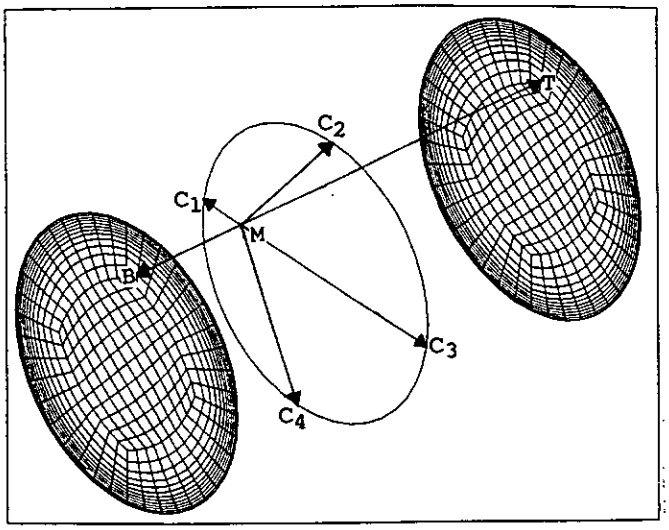

Figure 5. Calculation of the reference length δ.

On the injecting boundary, δ is assumed to be 0.05*D as for fully developped pipe flows. The continuity of δ, with the external flow, on the fluid-fluid boundary of the cylinder is ensured by the trilinear interpolation. A value of δ is assigned on the wall cylinder points by a linear interpolation based on the distances to the nearest points on the injecting boundary and on the fluid-fluid boundary. The values of the boundary layer thickness in the cylinder are determined from the values of δ on its boundaries in such a way that δ and therefore the eddy viscosity μ_t are continuous over the entire domain.

More precisely, for each point (M) inside the cylinder, multiple interpolation based on the distances to four points (C1,C2,C3,C4) distributed on the boundary circle and to two points (T,B), respectively on the top and the bottom of the cylinder, is performed to calculate the reference length δ (fig. 5).

The turbulent Prandtl number is maintained at the constant value 0.9.

Transition Modeling

In the transition zone ($s_S < s < s_E$), the eddy viscosity is modified by the intermittency factor γ, according to the Abu-Ghanam and Shaw (1980) theory :

$$\gamma = 1 - \exp(-5\eta^3)$$

with the nondimensional distance η

$$\eta = (s-s_S)/(s_E-s_S)$$

Initialization

The initial flow field results from interpolation of the flow variables between injection and downstream boundaries. Corrections are applied to have the flow tangent to the geometry and to simulate the near wall boundary layers. Inside the injection holes the initial flowfield is a combination of the flow induced by the injection boundary and the flow resulting from interpolation in the main stream. In other words, the blowing out of coolant air starts with the beginning of the iterative process.

ANALYSIS OF THE RESULTS

Flat Plate

The numerical results represent the well known phenomena occuring in a jet in a cross-flow.

The qualitative likeness, between experimental Laser tomography in different cross sections and calculated temperature distributions, is shown in figure 6. The kidney-shape, due to the contrarotating vortices, and the expansion of the jet are correctly predicted by the code.

More precisely, the code seems to predict the onset of the contrarotating vortices half a diameter upstream of the hole center (fig. 7). the experimental vectors describe a significant pair of vortices half a diameter downstream.

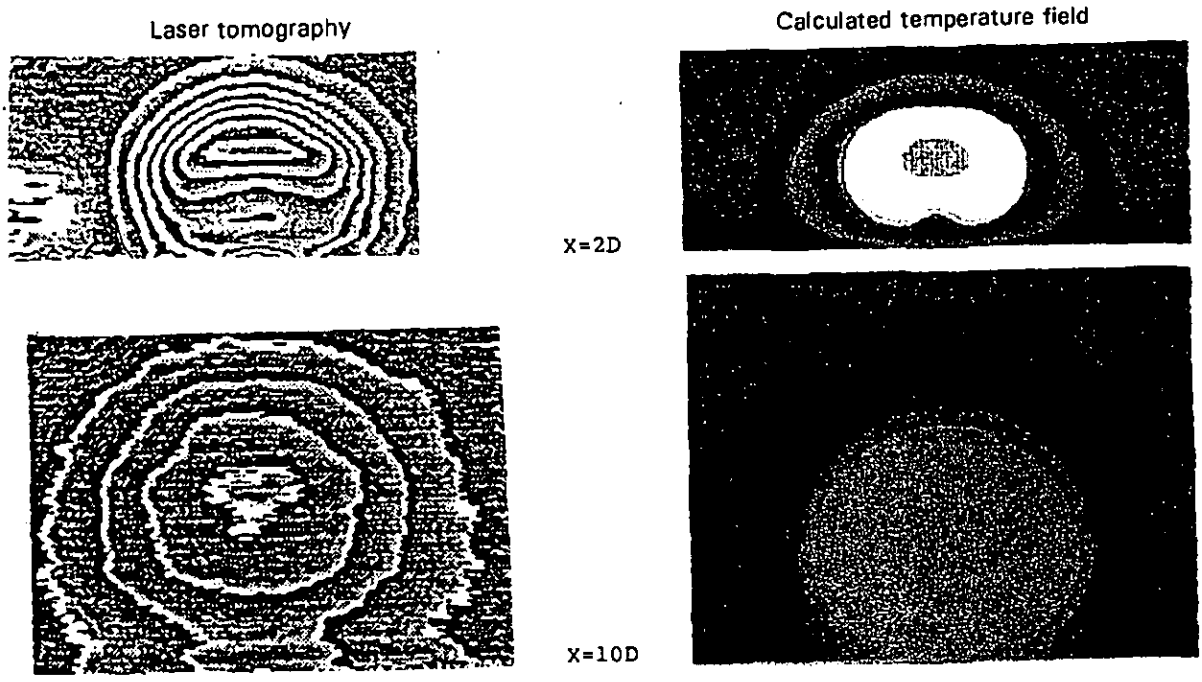

Figure 6. Qualitative comparison in different cross sections.

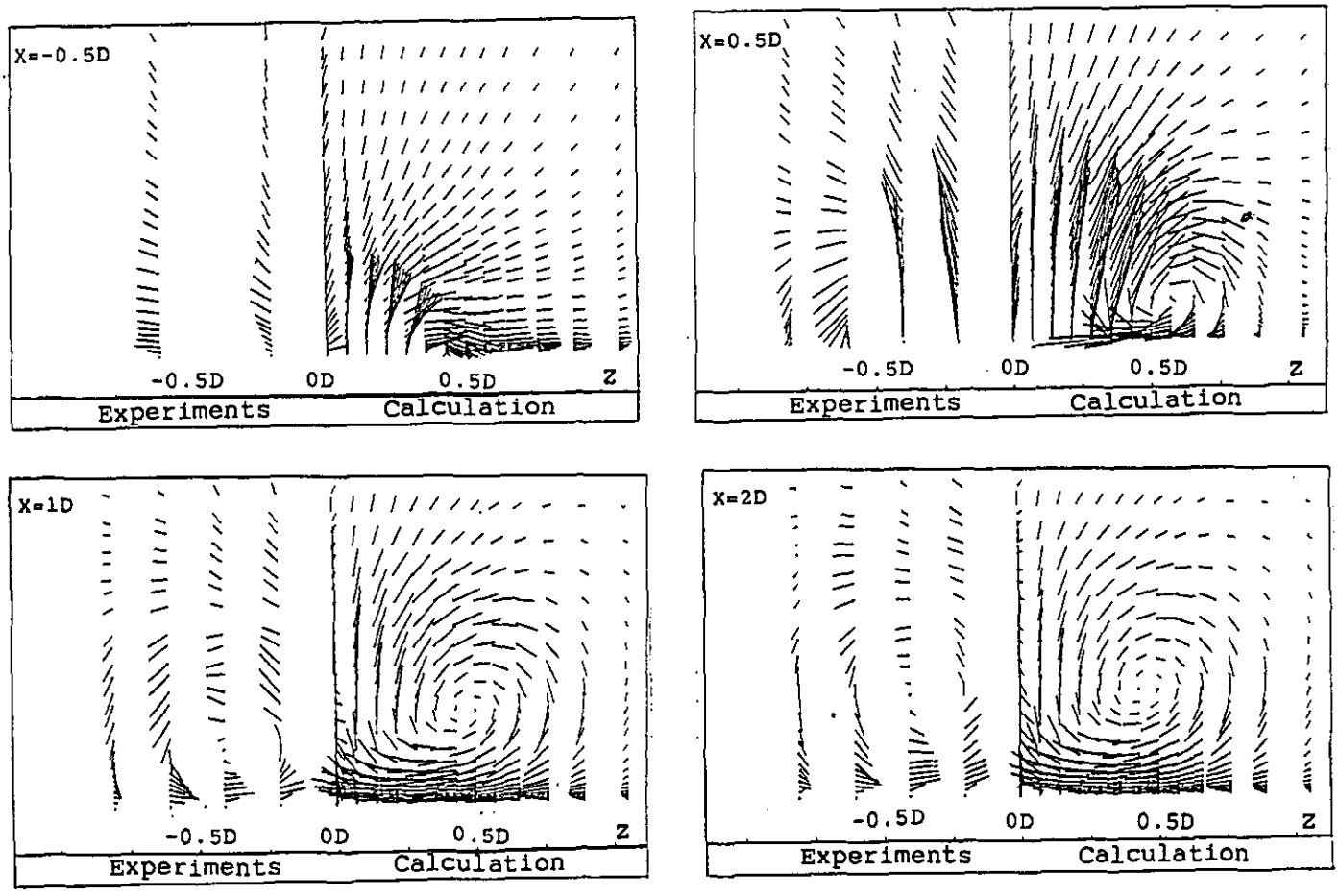

Figure 7. Velocity vectors in different cross sections.

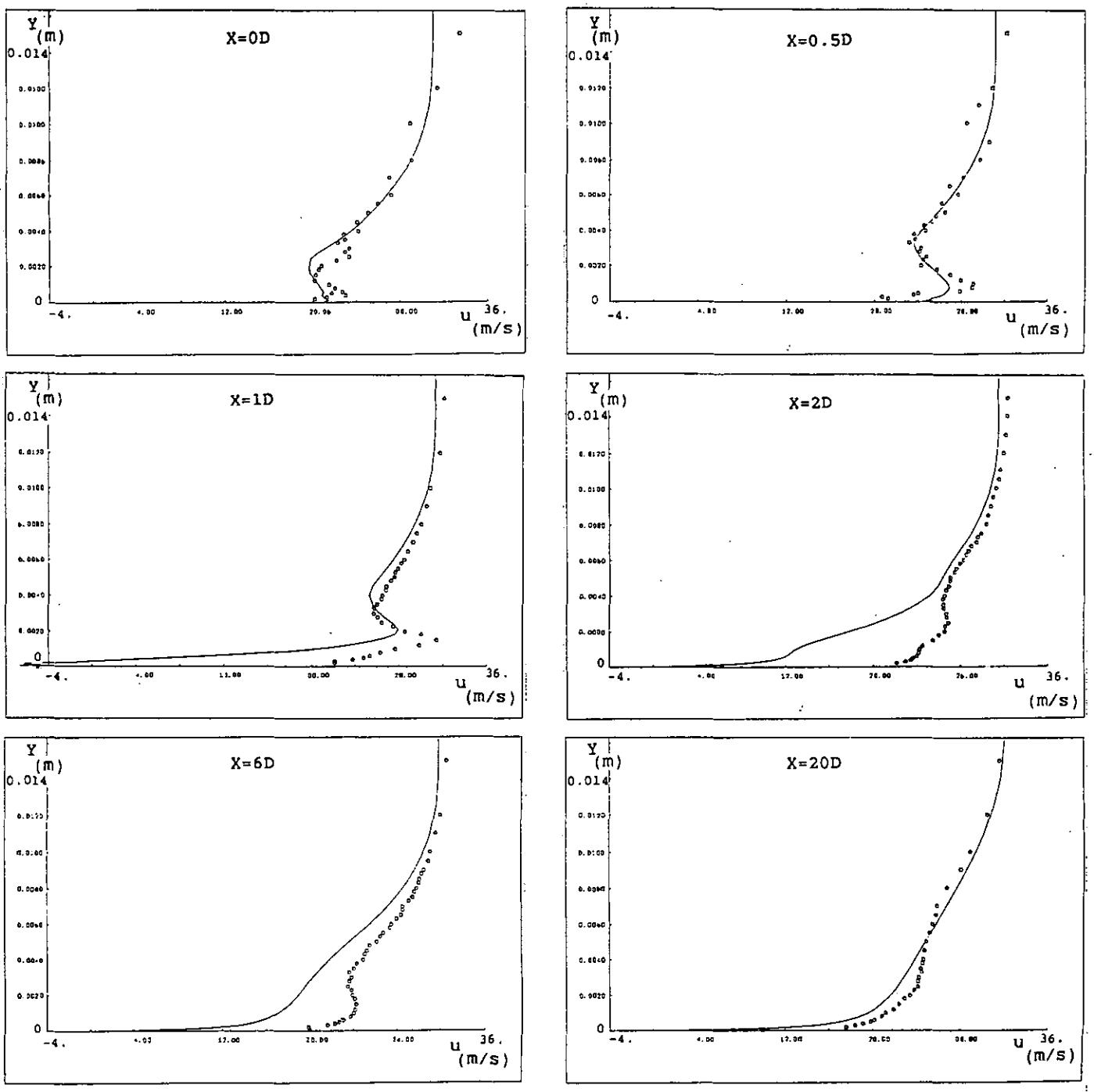

Figure 8. Longitudinal velocity profiles in the median plane (z = 0).

Consequently, the calculated vortex center trajectory lies above the experimental one. However, this gap has been totally reduced two diameters downstream and the intensity of the predicted vortices is close to the experimental one.

The examination of the longitudinal velocity profiles in the median plane shows, in the injection zone, a good agreement with the experiments (fig. 8, $0 < x < 2D$). However, large discrepancies appear beyond two diameters of the hole (fig. 8). The high longitudinal velocity region that lies near the wall is totally smoothed by the code during the iterations with the turbulence model (fig. 9 at 1000 iterations and fig. 8 at 3000 iterations).

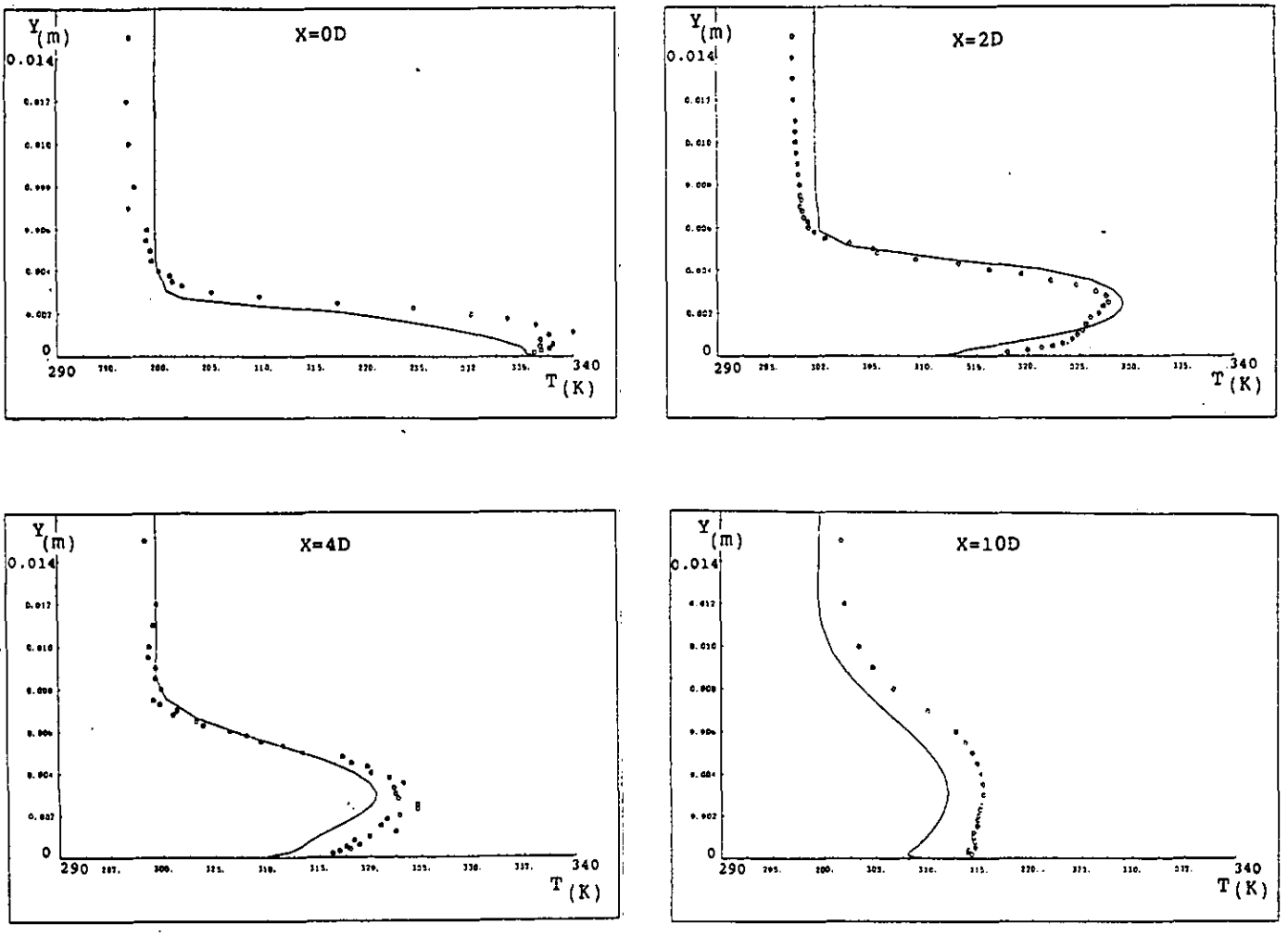

Figure 10. Temperature profiles in the median plane (z = 0).

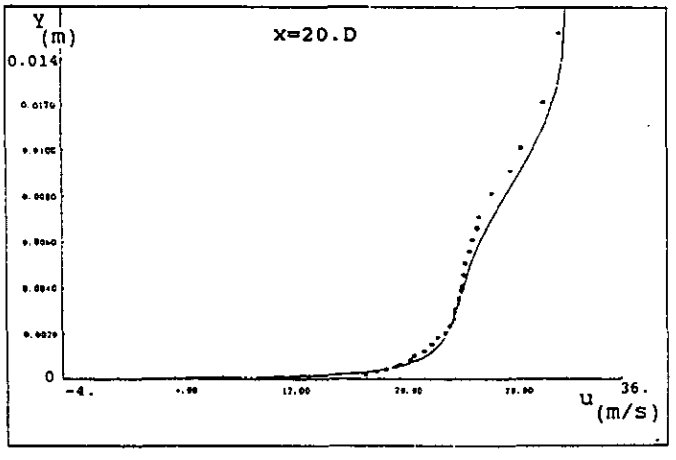

Figure 9. Longitudinal velocity profile in the median plane.

The turbulence in such flows could be anisotropic (Crabb et al., 1981) and the application of a mixing length turbulence model in the present computation may be inadequate. Moreover, using a mixing length turbulence model, the determination of a characteristic length in a case that combines a complex mixing of two different flows interacting with walls is far from a boundary layer case or a mixing layer of a wake flow.

Fair agreement was obtained between the computed temperature profiles and the experiments in the median plane (fig. 10). The gap, occuring on some profiles, between the main stream temperature of the experiments and the computed one, is due to the varying ambient conditions.

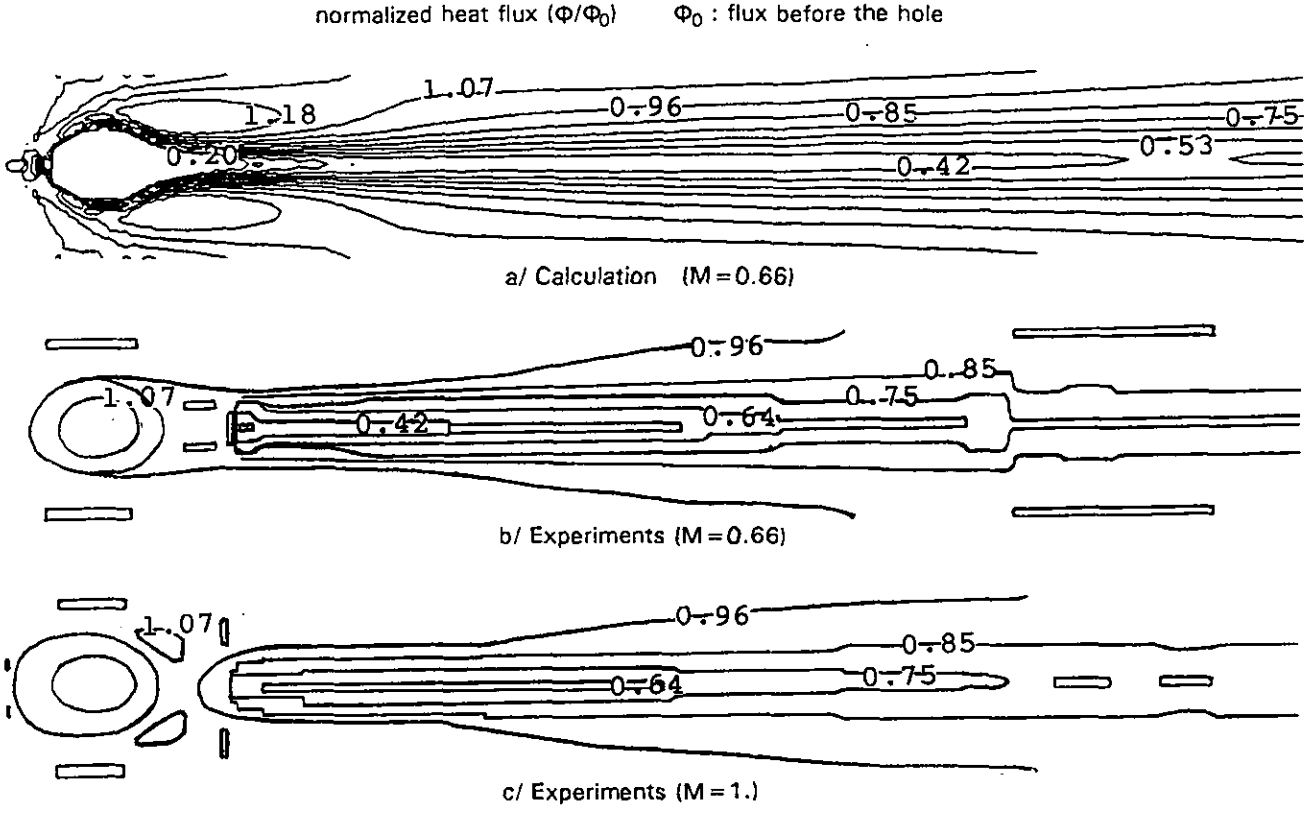

Figure 11. Heat flux on the flate plate.

The calculated heat flux, on the flat plate wall, shows good agreement with the experiments (fig. 11a and 11b). The region heated by the jet is as wide as the experimental results and confirms the good prediction of the jet expansion even near the wall. The over-estimation of the vortex intensity in the injection zone ($0<x<2D$) seems to generate the over-prediction of the heat transfer limited to the jet sides ($\Phi/\Phi_0=1.18$). Such a phenomenon is present in the experiments with higher blowing ratio ($M=1$)(fig. 11c, $\Phi/\Phi_0=1.07$) where the jet core is more compact.

These promising results obtained on a fundamental validation permitted testing the same code on a film-cooled vane airfoil.

Film Cooled Plane Nozzle Guide Vane

The operating conditions of this test have been described in table 1. The abscissae of transition have been imposed according with the significant increase of the experimental heat transfer coefficient in this zone. The abscissae of transition are on the pressure side and on the suction side :

$$s_S/s_{ps}=0.05 \quad s_E/s_{ps}=0.10$$
$$s_S/s_{ss}=0.16 \quad s_E/s_{ss}=0.26$$

The characteristics of the film-cooling jets described above for the flate plate are also available for this airfoil test case. However, the restitution of flow characteristics is less precise due to a relative slackened mesh, in the spanwise direction, with respect to the scale of these phenomena.

Total temperature in longitudinal sections, on the pressure and suction sides, shows the thin thermal boundary layer upstream from the injection zone and the development of the film cooling layer downstream (fig. 12a and 13a). The heat transfer coefficients on the wall represent the cooling effects of staggered holes (fig. 14). The jet emitted downstream is more efficient than the first one. A fundamental study, of such a cooling geometry on a flat plate at the CEAT-Poitiers, has shown this different behaviour of the two jets.

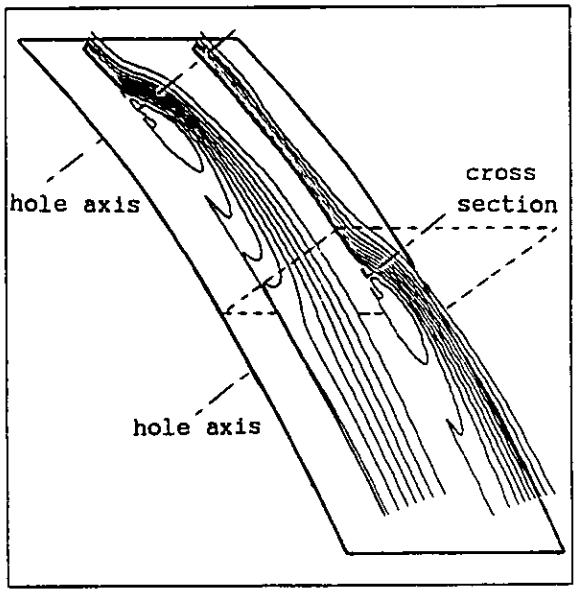

a/ Longitudinal sections passing by the hole centers.

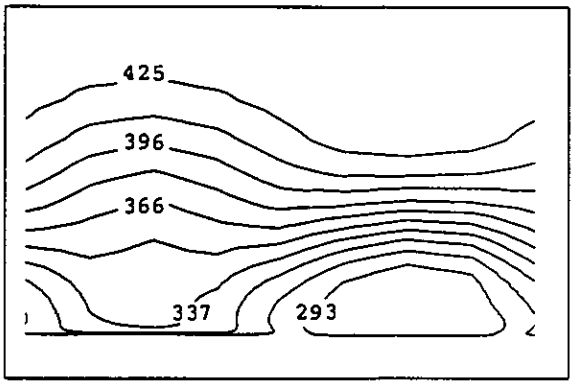

b/ Cross section one diameter downstream the second hole.

Figure 12. Total temperature (K) field on the suction side of the film cooled airfoil

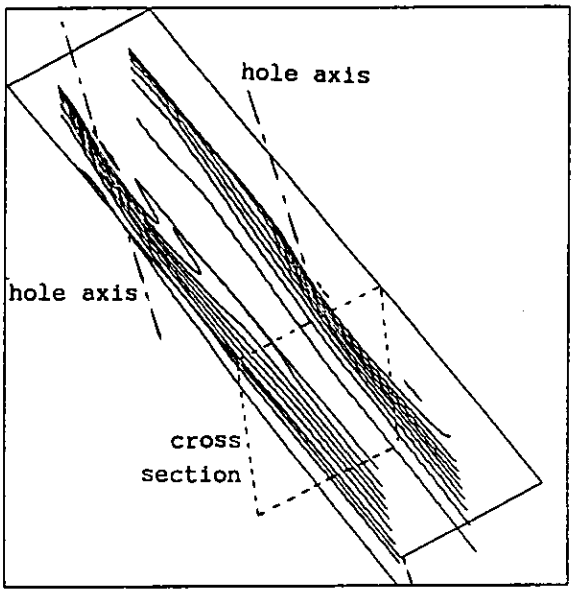

a/ Longitudinal sections passing by the hole centers.

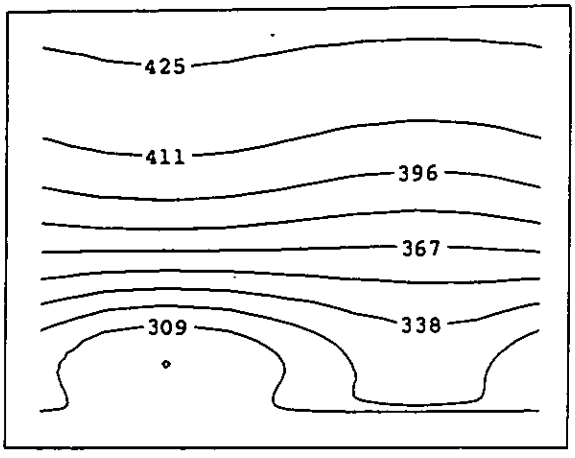

b/ Cross section one diameter downstream the second hole.

Figure 13. Total temperature (K) field on the pressure side of the film cooled airfoil

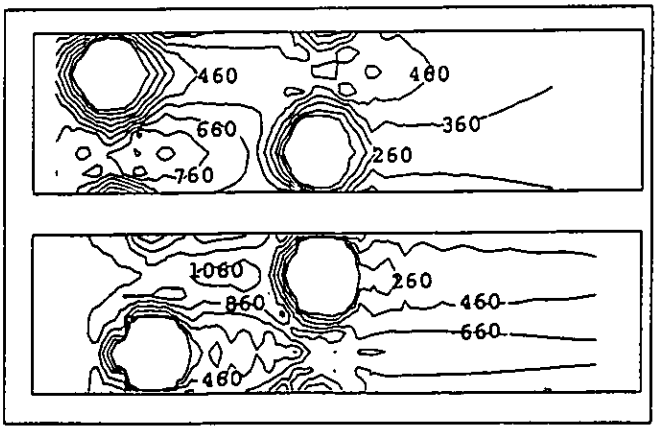

pressure side.

suction side.

Figure 14. Heat transfer coefficient (W/m²/K) on the wall airfoil in the injection zone.

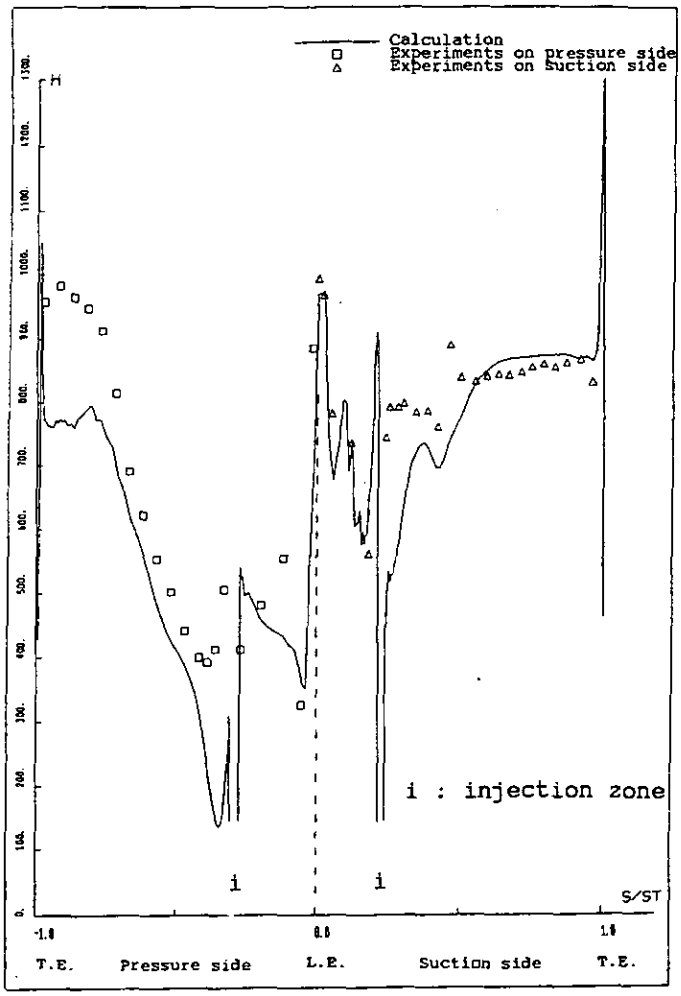

Figure 16. Span-averaged heat transfer coefficient.

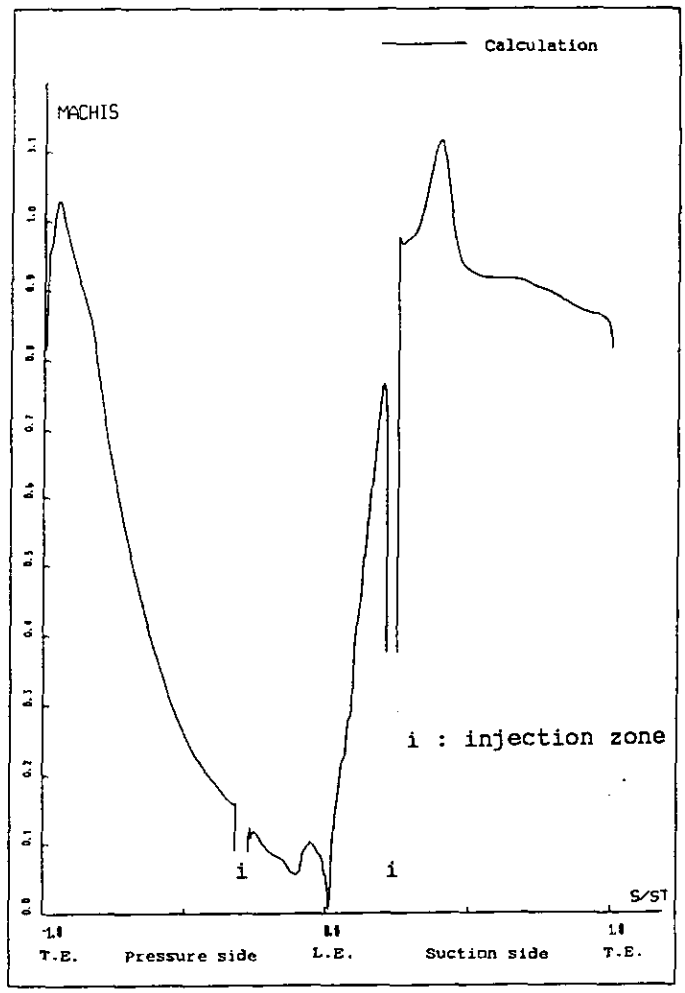

Figure 17. Span averaged isentropic Mach number.

Figure 15. Laser tomography one diameter downstream the second hole.
Two rows of staggered holes on a flat plate.

The trajectory of the first row jets (right side on figure 15), emitted upstream, lies above the second row jets (left side), emitted downstream (fig. 15). The jets of the first row seem to blow the jets of the second row against the wall (fig. 15, 12b and 13b).

The span averaged calculated heat transfer coefficient is compared to the experimental data on figure 16.

The results of the code are very sensitive to the mesh characteristics. The orthogonality of the near wall mesh is absolutely necessary. First calculations, with large regions of non orthogonal meshes, showed important over-estimation of the flux in these zones, though the points above the wall ensured a good value of y^+ ($y^+ < 1$).

The code represents a reasonable distribution of heat transfer coefficient, both on the pressure side and the suction side. The film cooling effect appears to be over-estimated in the injection zone, though the coolant mass flow is similar to the experimental one. A gap, between the calculated heat transfer coefficient and the experimental

one appears near the trailing edge on the pressure side ($-1. < s/s_{ps} < -0.8$). This lower estimation of the heat transfer corresponds with the transonic zone (fig. 17). The negative gradient of the velocity, after the shock impact on the suction side ($s/s_{ss} = 0.45$), seems to generate a flow seperation. The peak of the experimental heat transfer coefficient in this recirculation zone is not rendered by the code. The incomplete restitution of this phenomenon is probably due to an insufficient mesh refinement in this zone.

CONCLUSION

The calculation, of a hot jet in a flat plate turbulent boundary layer, has proved the capability of the code to predict the three dimensional flow and heat transfer on a fundamental test case. First application to a film cooled airfoil has shown the importance of the quality, refinement and orthogonality, of the mesh. The number of points necessary to compute these cases limits the application domain to one hole-pitch thick stream layer. Based on the results reported, various configurations of injection and geometry of holes can be now evaluated by the turbine blade designers.

ACKNOWLEDGEMENTS

This numerical study was supported by STPA. The authors would like to thank ONERA for the development of the solver and its fruitful cooperation. They are indebted to the CEAT-Poitiers staff, whose researches are financed by DRET, for their long standing cooperation and the quality of their experimental work. They appreciate the collaboration with the VKI and its documentation on film cooled test cases. They thank Miss Ritoux for her technical support. Lastly, the authors are indebted to Mr Lefebvre (student at Ecole Centrale de Lyon) and Mr Guénard (student at ENSICA-Toulouse) for their important contribution to this paper.

REFERENCES

Abu-Ghannam B.J. and Shaw R., 1980, "Natural Transition of Boundary Layers - The Effect of Turbulence, Pressure Gradient, and Flow History", *Journal Mechanical Engineering Science*, Vol. 22, No 5.

Ameri A.A. and Arnone A., 1991, "Three Dimensional Navier-Stokes Analysis of Turbine Passage Heat Transfer", *AIAA Paper* No. 91-2241.

Ameri A.A. and Arnone A., 1992, "Navier- Stokes Turbine Heat Transfer Predictions using two-Equation Turbulence Closures", *AIAA Paper* No. 92-3067.

Arts T. and Lapidus I., 1992, "Thermal effects of a coolant film along the suction side of a high pressure turbine nozzle guide vane", *Agard Conference Proceedings 527*, pp. 3.1-3.8.

Billonnet G., Couaillier V., Vuillot A.M. and Heider R., 1992, "Analysis of 3D Viscous Flow including Tip Clearance Phenomena in Axial Turbines", *Revue Française de Mécanique*, 1992-3 and -4.

Boyle R. and Giel P., 1992, "Three-Dimensional Navier-Stokes Heat Transfer Predictions for Turbine Blade Rows", *AIAA Paper* No. 92-306B.

Cambier L. and Escande B., 1990, "Calculation of a Three-Dimensional Shock Wave Boundary-Layer Interaction", *AIAA Journal*, Vol. 28, pp. 1901-1908.

Chanez P. and Petot B., 1993, "Viscous Analysis of High Pressure Inlet Guide Vane Flow Including Cooling Injections", *AIAA Paper* No. 93-1798.

Choi D. and Knight C.J., 1991, "Aerodynamic and Heat Transfer Analysis of a Low Aspect Ratio Turbine using a 3D Navier-Stokes code", *AIAA Paper* No. 91-2240.

Couaillier V., Grenon R. and Liamis N., 1992, "Transonic and Supersonic Flow Calculations around Aircraft using a Multidomain Euler Code", *13th International Conference on Numerical Methods in Fluid Dynamics*, Rome (Italy), July 6-10, 1992.

Couaillier V., Veysseyre P. and Vuillot A.M., 1991, "3D Navier-Stokes Computations in Transonic Compressor Bladings", *10th ISABE Symposium*, Nottingham, GB.

Crabb D., Durao D.F.G. and Whitelaw J.H., 1981, "A Round Jet Normal to a Cross Flow", *Trans ASME J. Fluids Engrg 103* pp. 142-153

Dorney D.J. and Davis R.L., 1993, "Numerical Simulation of Turbine 'Hot Spot' Alleviation using Film Cooling", *AIAA J. Propulsion and Power*, Vol. 9, No. 3, 329-336.

Fearn R. L. and Weston R. P., 1974, "Vorticity associated with e jet in a cross flow", *AIAA Journal*, Vol. 12, No. 12, pp. 1666-1671.

Foucault E., Deniboire P., Bousgarbiès J.L., Vullierme J.J. and Dorignac E., 1992, "Etude expérimentale du transfert de chaleur près d'une paroi plane chauffée en présence d'injections multiples", *Agard Conference Proceedings 527*, pp. 4.1-4.10.

Haas W., Rodi W. and Schönung B., 1991, "The Influence of Density Difference between Hot and Coolant Gas on Film Cooling by a Row of Holes: Prediction and Experiment", *ASME Paper* No. 91-GT-255.

Heider R., Duboue J.M., Petot B., Billonnet G., Couaillier V. and Liamis N., 1993, "Three-dimensional analysis of turbine rotor flow including tip clearance", *ASME Paper* No. 93-GT-111.

Jacquotte D.P. and Cabello J., 1988, "A Variational Method for the Optimization and Adaptation of Grids in Computational Fluid Dynamics", *Proceedings of the 2nd International Conference on Numerical Grid Generation in CFD*, Miami-Beach .

Kulisa P., Leboeuf F. and Perrin G., 1991, "Computation of a Wall Boundary Layer with Discrete Jet Injections", *ASME Paper* No. 91-GT-143.

Leylek J.H. and Zerkle R.D., 1993, "Discrete-Jet Film Cooling: a Comparison of Computational Results with Experiment", *ASME Paper* No. 93-GT-207.

Michel R., Quémard C. and Durand R., 1969, "Application d'un schéma de longueur de mélange à l'étude de couches limites turbulentes", *ONERA NT* No. 11.

Ni R.H., 1982, "A Multiple-Grid Scheme for Solving the Euler Equations", *AIAA Journal*, Vol. 20, No. 11.

Pietrzyk J. R., Bogard D. G. and Crawford M. E., 1989, "Hydrodynamic Measurements of Jets in Crossflow for Gas Turbine Film Cooling Applications", *ASME Journal of Turbomachinery*, Vol. 111, pp. 139-145.

Roth K.R., Fearn R.L. and Thakur S.S., 1992, "Evaluation of a Navier-Stokes Prediction of a Jet in Crossflow", *AIAA Journal of Aircraft*, Vol. 29, Number 2, pp. 185-193.

Wegener D., Le Meur A., Billonnet G., Escande B., Jourdren C., 1992, "Comparison Between two 3D-NS-Codes and Experiment on a Turbine Stator", *AIAA Paper* No. 92-3042.